Viper toxins affect membrane characteristics of human erythrocytes

Virjinia Doltchinkova [1*], Stoyl Stoylov [2] and Plamena R. Angelova [3]

[1] Department of Biophysics and Radiobiology, Faculty of Biology, Sofia University "St. Kliment Ohridski", 1164 Sofia, Bulgaria

[2] "Rostislaw Kaischew" Institute of Physical Chemistry, Bulgarian Academy of Sciences, 1113 Sofia, Bulgaria

[3] Department of Clinical and Movement Neurosciences, UCL Queen Square Institute of Neurology, London WC1N 3BG, UK

* *Correspondence to*: vdoltchinkova@gmail.com

Abstract: Elucidating electrokinetic stability by which surface charges regulate toxins interaction with erythrocytes is crucial for understanding the cell functionality. Electrokinetic properties of human erythrocytes upon treatment of Vipoxin , phospholipase A_2 (PLA_2) and Vipoxin acidic component (VAC), isolated from *Vipera ammodytes meridionalis* venom were studied using particle microelectrophoresis. PLA_2 and Vipoxin treatments alter the osmotic fragility of erythrocyte membranes. The increased stability of cells upon viper toxins is presented by the increased zeta potential of erythrocytes before sedimentation of cells during electric field applied preventing the aggregation of cells. Lipid peroxidation of low dose toxin-treated erythrocytes shows reduced LP products compared to untreated cells. The apparent proton efflux and conductivity assays are performed and the effectiveness PLA_2>Vipoxin>VAC is discussed. The reported results open perspectives to a further investigation of the electrokinetic properties of the membrane after viper toxins treatment to shed light on the molecular mechanisms driving the mechanisms of inflammation and neurodegenerative diseases.

Keywords: *erythrocytes, viper toxins, surface charge, lipid peroxidation, microelectrophoresis, proton transport, conductivity*

1. Introduction

Antimicrobial peptides have a widespread application as a key component of the immune defense systems. The activity of bee venom melittin is widely studied against microorganisms causing disturbance of membrane structure as a result of deformation and lipid extraction [1-3].Viper toxins as another type of antimicrobial peptides and model of toxins [4] are studied in order to clarify the biophysical characteristics of erythrocyte membranes during and after treatment. Important as structural models of membrane organization, erythrocytes carry negative surface electrical charge at physiological pH due to carboxyl groups of sialic acids in the cell membrane. This charge varies in different disease condition which can be determined by electrokinetic potential values [5]. The negative charges on the cells prevent erythrocyte aggregation and participate in immunohematological reactions [6]. Human erythrocytes of healthy adult subjects are characterized by 5 fractions of phospholipids: sphingomyelin, phosphatidylcholine, phosphatidylserine, phosphatidylinositol, phosphatidylethanolamine, and diacylglycerol. The erythrocyte membranes contain the following composition of phospholipids' fatty acids: myristic (14:0), palmitic (16:0), palmitoleic (16:1), stearic (18:0), oleic (18:1), linoleic (18:2), linolenic (C18:3), arachidic (C20:0), gondoinic (C20:1), eicosadienoic (C20:2) and behenic (C22:0) acids [7]. The erythrocyte membrane is composed of lipid domains exhibiting differential local mechanical properties which could depend on the specific lipid domain composition and on their differential association to membrane and cytoskeletal proteins [8]. The electrostatic charge of a cellular membrane has an important role in binding of multiple toxins to the cells [9, 10]. In view of their applications in prototypes of therapeutic agents [11-15], the physicochemical properties and interactions of toxic components with diverse model lipid systems or cells are investigated [16-18]. On the other hand, no reports are available regarding the surface properties of erythrocytes upon viper toxins treatment. Our rationale here was to study the relationship between the surface electrical charge and membrane characteristics of erythrocytes in the presence of viper toxins in order to elucidate their membrane stability. Viper toxins alteration of the membrane electrostatics is a result of

the generation of Van der Waals repulsive forces between the erythrocytes, preventing the aggregation of the cells. Changes in proton transport and conductivity characterize the permeability properties of the erythrocytes. The significance of lipid peroxidation of viper toxins-treated membranes reports for the reduced free radical products at low concentrations of toxins.

Solute movements across the erythrocyte membranes involve mainly the extracellular proton concentration (H^+_{ext}) in time, as well as the cotransport of Cl^- and H^+ and its antiport against other anions (OH^-) by the highly effective cycle of Jacobs-Stewart. According to the ionic states in erythrocytes, the existence of stable equilibrium (quazi - equilibrium "C" state) characterizes the permeability balance of all the anions and protons, keeping the preliminary content of Na^+ and K^+ [19]. The main role of Band 3 (AE1, SLC4A1) membrane protein in erythrocytes as an electro-neutral chloride/bicarbonate exchanger in alteration on the net surface charge is proposed. Band 3 is a dimeric glycoprotein and contains a 911 amino acid consisting of a N-terminal cytosolic domain (cdAE1, residues 1-360) responsible for the interaction with cytoskeleton and a C-terminal membrane domain (mdAE1, residues 361-911) responsible for its transport function [20]. Band 3 function may be regulated by lipids [21]. Determination of osmotic fragility and hematocrit on viper toxin-treated erythrocytes as a function of concentrations are essentially important for the functionality of the membrane [22, 23]. The present paper is concerned with electrokinetic and membrane transport studies of human erythrocytes in isotonic solution before sedimentation of erythrocytes in the presence of viper toxins.

The neurotoxin Vipoxin (*PDB: 1jlt/1aok*) is isolated from the venom of *V. ammodytes sp. meridionalis* - one of the most toxic snakes in Europe inhabiting only Balkan Peninsula. Vipoxin is a non-covalent ionic complex of two protein subunits: a basic and strongly toxic Ca^{2+} - dependent secreted phospholipase A_2 (GIIA-Asp49 $sPLA_2$), Vipoxin basic component to which further will be referred shortly as PLA_2 and an acidic, enzymatically inactive and nontoxic component, originally named Vipoxin acidic component (VAC) [24]. The vipoxin phospholipase A_2 (phosphatide-*sn*-2-acylhydrolase, PLA_2, EC 3.1.1.4) is one of the most

toxic phospholipases. By catalysing the hydrolysis of sn-glycero-3-phospholipids at the sn-2 ester bond, they release 1-lyso-phosphatidylcholine and a free acid, e.g. arachidonic acid, which takes part in the second messenger system cell signalling [25, 26]. Difference in the ionization behaviour of the various phenolic hydroxyl groups in the toxic PLA2 is reported: (i) three phenolic hydroxyls are accessible to the solvent and titrate normally, with a pK_{eff} = 10.45; (ii) three residues are partially 'buried' and participate in hydrogen bonds with neighbouring functional groups with a pK_{eff} = 12.17; (iii) two tyrosines with a pK_{eff} = 13.23 are deeply 'buried' in the hydrophobic interior of PLA_2 [27] According to Matsui and co-workers [28] venom of *Protobothrops flavoviridis Pfl*Lys 49-PLA_2 Basic Protein II harbours seven intramolecular disulphide bonds, thus 12% of the total 122 amino acids (14 Cys residues) contributes to covalent bond formation. Such a large number of intramolecular disulphide bonds may contribute to this unusual behaviour of this protein, i.e. oligomerization by a protein denaturant.

Cytoskeletal rearrangements in human red blood cells induced by snake venoms have been reported [29]. According to Vipoxin crystal structure investigations, the VAC and PLA_2 bind within their hydrophobic sides by complementary, well-fitted hydrophobic interactions and the complex is stabilized by electrostatic interactions between the positively charged PLA_2 and negatively charged VAC [30]. According to Devendjiev et al. [31] there is no evidence for the complex 'recognition site' involving residues Phe^{3}, Trp^{31} and Tyr^{119} of the molecules of VAC. In the PLA_2-subunit the side chains of His^{48}, Asp^{99} and Tyr^{52} for an active site which is conserved in all phospholipases [32]. The positively charged alkylammonium side chain of Lys^{69} may satisfy the need for partial neutralisation in the region of the structurally shielded Asp^{49} carboxylate in *Crotalus atrox* [33]. The ionic interaction between Lys^{69} (VAC) and Asp^{49} (PLA_2) in vipoxin complex is occurred. Vipoxin has a high affinity for biogenic amine receptors [34**].** According to these investigations, the VAC component and PLA_2 bind within their hydrophobic sides by complementary, well-fitted hydrophobic interactions and the complex is stabilized by electrostatic interactions between the positively charged PLA_2 and

115 negatively charged Acidic Component [30]. PLA_2 is a more hydrophobic substance
116 possessing 31 hydrophobic amino acids, but VAC is more hydrophilic agent with 24
117 hydrophobic amino acids. Furthermore, it is proposed that in the Vipoxin complex, VAC
118 component shields the access of substrate molecules to the active site of the enzyme thus
119 lowering the enzyme activity. Different roles are attributed to the VAC component but no
120 one is still proved as a result mainly from the diversity of pharmacological effects of the toxic
121 PLA_2 component.

122 Erythrocyte membranes exhibit a lipid-protein ratio of ~1 and negatively charged lipids and
123 proteins contribute to the total surface electrical charge of the cells. The lipid bilayer is the
124 basic structural element of membranes where a small amount of oxidized lipid is enough to
125 cause a drastic increase in phospholipid bilayer permeability [35]. Lipid peroxidation
126 produces a wide variety of oxidation products. Among the many different aldehydes which
127 can be formed as secondary products during lipid peroxidation, malondialdehyde (MDA) is
128 the most mutagenic product of lipid peroxidation [36]. MDA is used a convenient biomarker
129 for lipid peroxidation of omega-3 and omega-4 fatty acids because of its facile reaction with
130 thiobarbituric acid (TBA). However, the thiobarbituric acid reacting substances test
131 (TBARS) is applied for *in vitro* studies.

132 We demonstrate novel findings in the electrokinetic properties of viper toxins interaction
133 with the erythrocyte membrane. The biomacromolecules possess different effective
134 electrostatic charge of binding to the membrane. The surface properties of human
135 erythrocytes upon Vipoxin, PLA_2 or VAC are studied. We find that the electrokinetic
136 properties of the erythrocyte membrane upon viper toxin treatment, respectively, reflect
137 changes in their electrophoretic mobility (EPM) and the zeta potential of the cells as a marker
138 for stability of the erythrocytes. EPM changes are responsible for the dynamics of the surface
139 electrical charge and the extent of modification in membrane surface. Osmotic behaviour,
140 hematocrit and lipid peroxidation as convenient biophysical methods for cell functionality
141 status are used.The erythrocytes are highly susceptible to oxidative stress [37]. The

relationship between the enhancement of net surface charge and proton efflux and conductivity by viper toxins treatment is discussed. In order to determine the changes in free radical products and the mechanism of the protective effect of low doses of viper toxins in erythrocyte membranes is used. Viper toxins alter the shape of erythrocytes, proton transport and electrical conductivity due to the generation of lipid peroxides [38].

2. Materials and Methods

2.1. Materials

All chemicals used in the present study are of analytical grade. Neuraminidase (Vibrio cholerae, 5 U/mg enzyme); HEPES, N-(2-Hydroxyethyl) piperazine-N′- (2-ethanesulfonic acid); Na_2HPO_4, Sodium phosphate dibasic; KH_2PO_4, Potassium phosphate monobasic are purchased from Sigma-Aldrich (StLouis, MO) and the chemicals, as follows: $CaCl_2$, NaCl, KCl; trichloroacetic acid; 2-thiobarbituric acid (TBA); NaN_3, sodium azide; Sucrose. Bidistilled water from a quartz distiller for the preparation of all aqueous solutions is used.

2.2. Isolation and purification of the Vipoxin and its components

Isolation and purification of the Vipoxin and its components from the venom of the *Vipera ammodytes meridionalis* is described previously [39]. The two components of the Vipoxin (His-48 PLA_2 and Gln-48 PLA_2) after dissociation of the complex and purified are separated [40]**.** Vipoxin is isolated from a crude venom of Bulgarian nose-horned viper *Vipera ammodytes meridionalis* (Thracian Herpetological Society and National Centre of Infectious and Parasitic Diseases, Bulgaria) using ion-exchange chromatography on SP-Sephadex C-50 (Pharmacia, Sweden) according to the procedure described previously [41]. Data related to the purity of Vipoxin is presented in the supporting information (S1, Supporting Figure 1).

We have used the following viper toxin stock solutions: $sPLA_2$ (Mr 13800 Da, pI 10.4; 1.8 mg/mL) subunit, VAC (Mr 13740 Da, pI 4.6; 1.25 mg/mL) subunit and Vipoxin (Mr 27540 Da (5.3 mg/mL) and have done appropriate dilution of the toxins to 1:10 to 1:100 in the relevant buffer.

171 *2.3. Erythrocytes preparation*

172 Erythrocytes were prepared from citrate - containing blood from the blood bank of phenotype
173 A Rh^+ supplied by National Centre of Hematology and Perfusion in Sofia. Erythrocytes are
174 isolated after triplicate centrifugation with isotonic Hepes buffered saline and suspended in
175 the same buffer for microelectrophoresis measurements, ΔpH and conductivity analysis.
176 Erythrocytes were centrifuged (plasma and buffy coat removed) at 2000 x g for 5 min in a
177 microcentrifuge MIKRO 22R, *Hettich* (Germany), washed twice with isotonic Hepes
178 buffered saline: (25 mM Hepes, pH 7.5 (KOH),130 mM NaCl, 3.7 mM KCl, 0.25 mM
179 $CaCl_2$). We used the phosphate - buffered saline (PBS), containing 137 mM NaCl, 10.1 mM
180 Na_2HPO_4, 1.8 mM KH_2PO_4 for determination of hematocrit, osmotic fragility and lipid
181 peroxidation measurements, respectively, where the stock suspension of erythrocytes were
182 then diluted to 1% hematocrit.

183

184 *2.4. Hematocrit and osmotic fragility tests*

185 We determine the hematocrit (Hct) by microcentrifugation (NF 048 NÜVE SANAYI
186 MALZEMELERI IMALAT VE TICARET A.S bench-top centrifuge). Hematocrit
187 adjustment was performed by blood centrifugation (12500 x g for 2 minutes), plasma
188 removal and addition of cells in the desired ratio to obtain 20% (v/v). The samples aliquoted
189 into Eppendorf tubes and homogenized.

190 We used the osmotic fragility (OF) test at different concentrations of PLA_2, VAC or Vipoxin
191 to determine the degree of hemolysis. The erythrocytes osmotic fragility is fixed [42] by
192 adding erythrocytes to series of hypotonic solutions with decreasing NaCl concentration (0.9
193 % – 0.3 % NaCl, i.e., 0.154 M – 0.05 M NaCl) at 5% Hct, incubation for 30 min at 25 ^oC with
194 gentle mixing. Afterwards, 1.5 mL samples of the erythrocytes suspensions incubates with
195 toxin components at 25 ^oC for 30 min. The erythrocytes incubated with different hypotonic
196 solutions are then centrifuged (12000 x g for 1 min) after that the supernatants are removed.
197 The hemoglobin of each supernatant was measured using absorbance at λ=544 nm and λ=570
198 nm immediately after centrifugation [43] by means of a spectrophotometer Epsilon (Thermo

Fischer Scientific Inc., MA, USA). The OF_{50} (the concentration of NaCl that can induce hemolysis of erythrocyte cells by 50%) is calculated by plotting the relationship between absorbance at 544 nm or 570 nm, respectively, versus the concentration of NaCl solution.

$$H\% = \frac{\text{Abs } (\lambda)\text{in NaCl}}{\text{Abs } (\lambda)\text{in Viper toxins}} \text{ x } 100 \qquad (1)$$

Where $\text{Abs}_{(\lambda=544;\ \lambda=570)}$ in NaCl and $\text{Abs}_{(\lambda=544;\ \lambda=570)}$ in the presence of fixed concentrations of 50 nM (PLA_2, VAC or Vipoxin) are the absorbance of the release of hemoglobin into NaCl solution and Viper toxins containing media, respectively.

2.5. Treatment of erythrocytes with neuraminidase

For neuraminidase (EC.3.2.1.18) treatment, 0.5 mL of erythrocytes were suspended in 1 mL of Hepes buffered saline in the presence of 0.1 mL (10-50 mM IE) of diluted neuraminidase. The concentrations of neuraminidase of 25 nM, 50 nM, 80 nM and 100 nM PLA_2 were added and the suspension incubated for 60 min at 37 ^oC with constant gentle swirling. Control or 'Untreated' cells are suspended and incubated in a similar manner except no neuraminidase was added. There was a sample containing fixed dose of 25 nM PLA_2 without neuraminidase in the suspending medium.

Cells were washed with 1 mL of cold isotonic Hepes-buffered saline, pH 7.5 as above described immediately after completion of the incubation. Aliquots were taken for measurement of electrophoretic mobility. Samples (Ht 20%) were stored in refrigerator (4 ^oC) until use up to 4 h after erythrocyte preparation.

2.6. Microelectrophoretic measurements

Microelectrophoretic studies were performed in an OPTON Cytopherometer (Feintechnik Ges, mb. H, Germany), using a rectangular glass cell and platinum electrodes. The erythrocytes were diluted to 25 mL with Hepes buffered saline at 25 ^oC. The cells were observed under a light microscope connected to a video camera (Video Camera head CH

1400 CE, Sony corporation, Japan) providing 800 x magnification, which allowed migration by 20-40 cells to be timed.

The zeta potential,ζ i.e. the electrostatic potential at the hydrodynamic shear plane [44], is calculated from the value of the EPM, u by the Helmholtz-Smoluchowski equation:

$$\zeta = \frac{\eta u}{\varepsilon_r \varepsilon_0} \quad (2)$$

where ε_r is the relative dielectric constant of the aqueous phase ($\varepsilon_r =$ 78.5 at 25°C), η denotes the viscosity of the aqueous phase (25 mM Hepes buffer, 130 mM NaCl, 3.7 mM KCl, 0.25 mM $CaCl_2$, pH 7.5; $\eta =$ 1.21 ± 0.02 mPa.s), ε_0 stands for the vacuum permittivity (ε_0= 8.8542.10^{-12} F.m^{-1}) and EPM is expressed in value u.10^8 m^2.V^{-1}.s^{-1}. Values represent the mean of tree – seven replications. The standard error of mean is between 2 and 5 %.

The surface electrical charge (σ) reads:

$$\sigma = A^{-1}(C_{i\alpha})^{1/2} \sinh(Z\psi_0/51.38) \quad (3)$$

where$A = 1/(8N_A\varepsilon_r\varepsilon_0 T)^{1/2} = 136.6$ at 25°C, $N_A = 6.022 \cdot 10^{23}$mol^{-1} is the Avogadro number,$\psi_0 \approx \zeta$; σexpresses in C m^{-2} [45].

For experiments designed to assess membrane physico-chemical properties, 25 µL of erythrocyte preparation was resuspended in 0.5 mL of Hepes buffered saline to a final density of 4.5x10^{6}cells/mL. Erythrocyte suspension was diluted into the 25 mL isotonic Hepes buffered saline tubes containing 2.2x10^6 cells/mL in the EPM measurements. Control erythrocytes contain isotonic Hepes buffered saline devoid of viper toxin.

2.7. Lipid peroxidation: Detection of malondialdehyde (MDA) content

The malondialdehyde content was evaluated by analysis of thiobarbituric acid reactive substances (TBARS) [46] with some modifications. Erythrocyte suspension was centrifuged three times at 4500×g using MiniSpin ® microcentrifuge (Eppendorf, Germany) for 4 minutes in 1 mL of the PBS solution at pH 7.4. The pellet was re-suspended with 500 µL PBS solution to Hct 20% and dilutes to 10 mL PBS, pH 7.4, containing 2 mM NaN_3. Immediately afterwards, 500 µL of erythrocyte suspension was incubated with the

corresponding concentration of PLA_2 at 37°C for 5 minutes or 30 minutes, respectively and diluted to 1 mL of the PBS buffer. The sample of erythrocyte suspension without PLA_2 represents the control values. The second control with 50 mM H_2O_2 is prepared and the maximal content of lipid peroxidation is registered. In a second set of experiments where the lipid peroxidation of erythrocytes was measured in the presence of fixed doses of 50 nM concentrations of viper toxins. The control sample without viper toxins was incubated at 37 °C for an hour in PBS solution, pH 7.4.

After incubation of erythrocytes without or in the presence of viper toxin, 0.4 mL of 28% trichloroacetic acid was added to the suspension. The following centrifugation at 12500×g for 2 min at 4 °C is made. One mL of the reaction mixture and 0.5 mL of 1% thiobarbituric acid were incubated at 95 °C for 30 min. The suspending medium is centrifuged at 12 500×g for 2 min, and the absorbance of λ=532 nm is measured by means of a spectrophotometer Epsilon (Thermo Fischer Scientific Inc., MA, USA) to determine the MDA content. TBARS molar concentration, *c*, is calculated:

$$c = \frac{A}{\varepsilon l} \qquad (4)$$

where A is the absorbance, ε stands for the molar absorption coefficient of H_2O_2, $\varepsilon_{532} = 154000\ M^{-1}cm^{-1}$, l represents the optical path length. The lipid peroxidation of erythrocyte membranes is estimated by the production of thiobarbituric acid reactive substances (TBARS) and expressed in M cm^{-1}[46].

2.8. Measurements of proton transport and conductivity

The experimental study on the anion-proton co-transport bases on the measurement of net proton flows associated with Band 3-mediated net anion transfer. Erythrocytes suspended in hypotonic sucrose salt-free solution were characterized by the exchange of inorganic anions of chloride and carbonate in connection with the pH equilibration which occurs in minutes. Water transport equilibrates the osmotic gradient in less than one second [19]. A case of "C-state" for erythrocytes is described, where a quasi-stationary state is stable for hours if the membrane permeability is not artificially altered. In the latter processes the osmotic equilibrium, the pH and the anion concentration were equilibrated. The distribution of ions

279 which are in equilibrium with the outside ionic concentrations are described according to the
280 Nernst equation where the activity of the corresponding ion from the interior represents the
281 exponential function of the charge of the ion from the exterior multiplied by the electric
282 potential difference.
283 We measured the extracellular proton concentration (H^+_{ext}) as a function of time in seconds
284 promoted by the treatment of erythrocytes with viper toxin components [47]. The suspending
285 medium of 0.3 M sucrose (NaOH), pH 7.4 was used to maintain its buffer capacity constant
286 over the pH range covered in the experiments [19]. Proton efflux and electrical conductance
287 begin by mixing of 100 µL of erythrocytes suspended into 50 mL of 0.3 M sucrose (NaOH),
288 pH 7.4. The pH and conductivity of the erythrocyte suspension without or in the presence of
289 different concentrations of viper toxins were measured using a Thermo Fisher Instruments
290 Pte Ltd., (USA/Singapore) pH/conductivity meter.
291 The results for the proton efflux alteration in extracellular media in the presence of different
292 concentrations of toxins is obtained from membrane transport measurements in suspending
293 media every 20 s during 5 minutes at gentle mixing. The value of $\Delta pH(\%)$ is calculated
294 from:

$$\Delta pH = \frac{(pH_o - pH_t)}{pH_0} \; x \; 100$$

295 where pH_o and pH_t are the pH values of erythrocytes in toxin-free medium and in the
296 presence of toxin concentration, respectively. The slope of linear fit ΔpH curve represents
297 the rate of the reaction.
298
299 *2.9. Statistical analysis*
300 The data obtained in the experiments are expressed as mean ± SD from the 3-7 independent
301 measurements. The significant means are determined by use of ANOVA after 3 repetitions.
302 The data are analyzed by the use of One-way analysis of variance with
303 Student-Newman-Keuls method for all pairwise comparisons on the mean responses among
304 the different groups taking $p \leq 0.05$ as significant. Dunn's test for all pairwise comparisons

and comparisons against a control group following rank-based ANOVA as well as Holm-Sidak test for both pairwise comparisons and comparisons versus a control group was also used.

3. Results

3.1. Osmotic fragility and hematocrit

Figure 1 represents the results for the osmotic fragility (OF_{50}) in the presence of fixed concentrations of PLA_2, VAC and Vipoxin, respectively as obtained from osmotic fragility at suspending media with different NaCl concentrations. The value of ΔOF (50%) is calculated:

$$\Delta OF = \frac{\left(OF_{Vipertoxin} - OF_0\right)}{OF_0} \; x \; 100$$

where $OF_{Vipertoxin}$ and OF_0 are the osmotic fragility of erythrocytes in the presence of the Viper toxin and in Viper toxin-free medium, respectively.

Data about hematocrit determination as well as osmotic fragility (OF_{50}) under toxins treatment are characterized by 30 min time period according to the protocols described. After 50 nM PLA_2 treatment, the fragility of erythrocytes increases strongly at 570 nm, where the H_{50} = 0.7% NaCl is observed (p=0.002, Figure 1A). The enhancement in Hct of erythrocytes in the presence of 50 nM PLA_2 compared to control is shown on Figure 1B (p=0.004). Vipoxin (50 nM) leads to an increase in OF_{50} at 544 nm (p=0.002) without a significant change in Hct. There is change in OF_{50} of erythrocytes treated by 50 nM VAC at 544 nm (p=0.021).

3.2. Electrokinetic properties of erythrocytes in the presence of Neuraminidase

We test the electrokinetic behaviour of erythrocytes in the presence of neuraminidase (NU) to determine the electrophoretic mobility compared to EPM of untreated erythrocytes. The erythrocyte membranes are treated by neuraminidase (which removes charge bearing sialic acid) for 2 hours at 37 ºC. The PLA_2 treatment shows no activity on EPM of erythrocytes

under neuraminidase pre-exposure sample compared to control after incubation (2 hours at 37 ^{o}C), but increases the EPM of PLA_2 treated erythrocytes compared to the control without incubation (Figure 2A). The erythrocytes velocity upon PLA_2 treatment delays in an electric field, while the aggregate complexes of erythrocytes did not allow for measurement due to electrostatic attraction of uncharged surfaces, only the sharply-looking NU-treated erythrocytes were observed and timed ($p=0.013$).

Erythrocyte suspensions without or in the presence of different concentrations of neuraminidase were prepared. Pre-incubated with NU erythrocytes (for 1 h at 37 ^{o}C) were treated by PLA_2 at the same conditions as in the case of control human erythrocytes (Figure 2B). The results show that after the process of the pre-incubation with NU erythrocytes alter its electrokinetic parameters (electrophoretic mobility and zeta potential) upon PLA_2 treatments. It was registered that the treatment by pre-incubation with 30 mU, 40 mU and 50 mU neuraminidase the erythrocyte membranes possess lower zeta potential compared to the sample without neuraminidase treatment of erythrocytes after the incubation for 1 h at 37 ^{o}C ($p<0.001$, Figure 2B).

There was a decrease in zeta potential of erythrocytes upon 25 nM PLA_2 application ($p<0.001$). A decrease in EPM of erythrocytes pre-incubated with 20 mU NU is characterized by swelling of the cells in the presence of 25 nM PLA_2 in suspending medium. PLA_2 induces aggregation upon pre-incubated with 30 mU NU and aggregate formations of erythrocyte suspension at the first minutes of treatment. There is a settlement of erythrocytes upon 25 nM PLA_2 in neuraminidase pre-incubated erythrocytes due to the structural changes of the membranes. Increasing the concentration of PLA_2 to final concentration of 50 nM PLA_2 leads to a settlement and rupture of erythrocytes and its aggregation after 7 minutes. There is a significant difference in zeta potential of erythrocytes pre-incubated with 30 mU neuraminidase and 50 nM PLA_2 ($p<0.001$). Exposure of erythrocytes to 40 mU NU causes formation of a different fractions of erythrocytes in suspending medium – smaller cells, swelling and normal discocyte forms. PLA_2 treatment (25 nM) induces swelling of erythrocytes and aggregation in part of them.

As previously noted, the aggregated erythrocytes were not measured. Addition of 50 nM PLA_2 induces a less negative EPM of erythrocytes during movement in an electric field, where swelling, lysis and aggregation of part of the cells are observed. Erythrocytes pre-incubated with 40 mU NU show reduction of the zeta potential compared to the control erythrocytes ($p<0.001$, Figure 2B). Higher concentrations of PLA_2 (80 nM) induce higher zeta potential than the pre-incubated with 40 mU NU cells. Pre-incubated with 50 mU NU erythrocytes possess a decreased EPM compared to the control samples. Swelling of part of the erythrocytes was observed. PLA_2 treatment of pre-incubated with 50 mU NU erythrocytes led to aggregation of some of the spherocytes at the first minute after 25 nM PLA_2 exposure and structural changes could be promoted.

3.3. Electrokinetic properties of erythrocytes in the presence of viper toxins

Microelectrophoretic observations show novel results about the electrokinetic properties of erythrocytes during 5-7 minutes measurements of erythrocyte membranes in the presence of viper toxins. The affected cells change their typical shape of biconcave disks to a spherical form. The results show that the disruption follows a 2-3 μm bleb formations changing the organization of the cell structure. The electrostatic effect of PLA_2 is expressed on the erythrocyte membrane. A blebbing effect and large disruptions of the membrane were reported on model lipid membranes [48]. Vipoxin promotes a similar effect to the effect of PLA_2 on the erythrocyte membranes and a blebbing effect at higher concentrations of treatment was observed. Viper toxin components represent multivalent membrane-associating molecules with an 'effective' charge for adsorption to the membrane to proceed at an interface, not within the diffuse ionic double layer. Vipoxin, PLA_2 and VAC have an effective charge of +3.8, +4.3 or of +3.3, respectively in pH 7.5 at ionic strength $I=0.1\ M^{-1}$ [49].

Erythrocytes possess a zeta potential of $\zeta = -20$ mV in isotonic suspending medium. Our results show an enhancement of negative zeta potential with 3.7 mV at 10 nM Vipoxin or at 50 nM Vipoxin in suspending medium and a higher increase of 5.5 mV in ζ potential at

dose of 100 nM Vipoxin ($p<0.001$) in comparison to untreated erythrocyte cells (Fig. 3A). We suggest that Vipoxin enhances the magnitude of the negative electrostatic surface potential and increases the electrostatic binding of positively charged residues on its macromolecule to the membrane surface.

PLA_2 changes significantly the ζ potential of erythrocyte membranes at concentration of 10 – 100 nM of treatment (Fig. 3B). A decrease in zeta potential of erythrocytes upon 50 - 100 nM PLA_2 was observed.

VAC at 50 nM significantly alters the EPM, zeta potential and surface charge compared to the untreated erythrocyte suspension. Zeta potential of erythrocytes upon the 50 nM VAC treatment possesses values of $\zeta = -28.3$ mV in comparison to the erythrocytes without VAC (Figure 3C). Higher concentration of VAC, 80 nM, reduces the zeta potential ($p=0.001$) of erythrocyte suspension, compared to the untreated control.

Surface electrical charge of erythrocytes is characterized by $\sigma = -0.0264$ C m^{-2} in the presence of fixed concentration of 50 nM VAC in suspending medium compared to control sample of $\sigma = -0.0181$ C m^{-2} without VAC (Figure 4). Exposure to 50 nM Vipoxin shows a lower value of $\sigma = -0.0211$ C m^{-2} than the value of surface charge at the same concentration of VAC in erythrocyte suspension (Figure 4).

3.4. Lipid peroxidation of erythrocytes in the presence of the Phospholipase A_2

We studed the hydrogen peroxide content at the plasma membrane of erythrocytes upon viper toxin treatments. Hydrogen peroxide (H_2O_2) is produced endogenously in a number of cellular compartments, including the plasma membrane, where it can play divergent roles as a second messenger or a pathological toxin [50].

Phospholipase A_2 concentration ranges from 50 nM – 1000 nM alter lipid peroxidation status of erythrocyte membranes for a longer time of treatment (30 min) ($p<0.001$). Short time incubation (5 min) of 50 nM – 1000 nM PLA_2 with erythrocytes significantly alters the concentration of free radicals in living cells (Figure 5A, $p<0.001$**),** differentially. There is a strong increase in TBARS values of erythrocytes in the presence of 50 nM PLA_2 for

both times of incubation. The reduction of lipid peroxidation of erythrocyte membranes is determined with increasing the dose of treatment with PLA_2 for shorter time of incubation. Doses of 100 nM PLA_2 and 1000 nM PLA_2 in erythrocyte suspension induce a maximal enhancement of TBARS levels after 30 min time of incubation.

A reduction of the lipid peroxidation of erythrocytes upon fixed concentrations of 50 nM Vipoxin, PLA_2 and VAC was observed (Figure 5B). The 50 nM PLA_2 has no effect on lipid peroxidation of erythrocytes compared to the TBARS value of untreated erythrocyte membranes. VAC and Vipoxin decreased the lipid peroxidation levels of erythrocyte suspension by a similar extent ($p=0.007$) in comparison to the TBARS of control erythrocytes without VAC or Vipoxin, respectively. Lipid peroxidation of erythrocyte membranes in the presence of 50 mM H_2O_2 showed highest value of 1.1 µM TBARS after 1 h incubation of erythrocytes compared to control- viper toxin free-treated cells.

3.5. Membrane transport and conductivity measurements

Membrane transport test monitors the proton efflux from the erythrocytes suspended in sucrose salt-free medium. Extracellular proton concentration (H^+_{ext}) as a function of time is changed by the treatment of erythrocytes by viper toxin components. Figures 6 (A,B) and 7 (A,B) represent the results for the proton efflux alteration in extracellular media in the presence of different concentrations of toxins as obtained from membrane transport measurements in suspending media every 20 seconds during 5 minutes at gentle mixing. Figures 6 (C,D) and 7 (C,D) describe the conductivity of erythrocyte suspension in the presence of viper toxins.

PLA_2 induces an increase in the slope of the linear fit curve of ΔpH (10 – 60 nM) (Figure 6B) and the slope of conductivity linear fit at dose of 20 nM (Figure 6D). In order to study the mechanism of interaction of fixed concentrations of 50 nM viper toxins with erythrocyte membranes, the ΔpH measurements were performed at different times. The maximum value of the proton concentration in extracellular space of erythrocytes in the presence of 50 nM PLA_2 is reported on Figure 7B. A dose of 50 nM PLA_2 slightly changed

443 the H^+ efflux, but strongly altered the conductivity of erythrocyte suspension. A strong
444 increase in the slope of conductivity of erythrocyte suspension upon basic Vipoxin
445 component was measured (Figure 7D).
446 VAC induces a decrease in the slope of the linear fit curve and lower value of the proton
447 concentration in extracellular space in erythrocytes due to the lower pI of the acidic
448 component in comparison to the control kinetic curve (Figure 7B). VAC increases the H^+
449 efflux up to 140 s after beginning of the membrane transport registration, but accompanied
450 by a strong enhancement of conductivity in all times measured (Figure 7D).
451 Vipoxin inhibits the slope of linear fit curve of ΔpH registration up to 20 s, after that the
452 processes of transport of protons is characterized without changes in the H^+ efflux but
453 increases the conductivity of the erythrocyte suspension compared to control values (Figure 7
454 B, D).
455

456 **4. Discussion**

457 Viper toxins strongly affect the membrane characteristics of erythrocytes. The reported
458 biomacromolecules are of deep interest under various pathophysiological conditions. In the
459 present study, we investigate the interaction of viper toxins with erythrocyte membranes the
460 using the electrokinetic approach. VAC and Vipoxin both possess similar effective
461 electrical charges on their molecules and induce an increase in negative surface electrical
462 charges on the erythrocyte membrane due to an electrostatic interaction with erythrocyte
463 membranes. In our experiments we use low treatment concentrations of viper toxins in
464 order to prevent aggregation of erythrocytes due to disruption of cells and following
465 sedimentation of erythrocytes during microelectrophoretic measurements at 52 nM PLA_2 in
466 suspending medium. Higher concentrations of PLA_2 decrease the zeta potential of the
467 erythrocytes due to the effect of Ca^{2+} in suspension medium on the activity of PLA_2. Zeta
468 potential of human erythrocytes increases with increasing Vipoxin concentration promoted
469 by their binding to the membrane. More negatively charged surface by Vipoxin and VAC
470 treatments on the outer surface of the erythrocyte membrane determines the higher surface
471 electric charge where electrostatic forces of repulsion dominate over attraction between the

erythrocytes. The upper effect is due to the contribution of Band 3 negative charges on the dimeric interface of the membrane upon viper toxin treatments on the erythrocytes [21].

Our results show that neuraminidase pre-treated erythrocytes do not change their electrokinetic properties, evoked by the PLA_2. Neuraminidase diminishes the net surface charge of the membrane and ζ potential values of erythrocytes do not change appreciably when treated with various toxins. The untreated erythrocytes possess lower net negative charge compared to erythrocytes incubated with neuraminidase for an hour at 37 ^{o}C. Our results show that neuraminidase does not exhibit a hemolysis of erythrocytes. Despite the action of PLA_2 on erythrocytes for longer time of incubation, NU pre-incubation causes an increase in EPM and zeta potential on the membrane. Hence, the sialic acid residues are not the main factor in determining the electrokinetic properties of erythrocyte membrane upon PLA_2 action on the membrane. The externalization of the negatively charged phospholipids from the inner membrane due to formation of products of the phospholipase reaction upon viper toxin application results from the local damage of the membrane. The phospholipase A_2 activity is increased in vesicles containing oxidized soybean phosphatidylcholine compared that the activity in non-oxidized phospholipid membranes [51]. According reports of Litvinko et al. [52] PLA_2 does not act on the tightly packed lipid bilayers. The exposure of additional negative charged groups of the proteins and lipids on the surface of erythrocytes because of conformational changes and re-organization of membrane components explains the higher net surface charge of erythrocyte membrane upon viper toxin treatment.

The interactions of anionic phospholipids and cholesterol and specific sites of Band 3 are situated at the dimeric interface forming and annulus around the protein. The upper strong interactions may play a role in folding and function of this anion transport membrane protein [21]. PLA_2 influences the membrane transport and conductivity of erythrocyte suspension. Lower concentration of PLA_2 (1 nM) leads to a reduction of the rate of proton efflux. It is demonstrated in an indirect relationship with the inhibition of membrane transport at the side of the transmembrane protein of Band 3 for proton and H^+ /Cl^-

cotransport across the erythrocyte membrane without changes in conductivity. On the contrary, higher concentrations of PLA_2 (20-60 nM) had no alteration on the anion-exchange function of Band 3, without change in H^+ efflux, but with a strong increase in conductivity of erythrocyte suspension. PLA_2 promotes an enhancement of the concentration and mobility of the ions in erythrocyte suspension without changing the proton efflux at 20-60 nM doses due to an increased production of free radicals, especially lipid peroxides. There is a higher MDA content of erythrocyte membrane in the presence of 50-100 nM PLA_2 for a short time of incubation compared to the untreated erythrocytes.

Fixed concentrations of 50 nM PLA_2 induce an increase in the rate of the proton efflux through the membrane and strong enhancement of the conductivity of erythrocyte suspension. The VAC leads to a strong reduction in the rate of the proton efflux and increase in conductivity perhaps by restricting the conformational change in Band 3 that occurs during transport. VAC induces more negatively charged groups of the C-terminal membrane domain of Band 3 to be exposed and follows a large enhancement of net surface charge. In the case of 50 nM VAC treatment an increase in negative charges on the membrane surface is a result of the electrostatic interaction of its macromolecules with negatively charged membranes leading to Van der Waals repulsive forces between the VAC-treated erythrocytes. The fixed doses of 50 nM Vipoxin causes the higher surface electrical charge and conductivity because of the reduction in the rate of the H^+ efflux in the extracellular space.

The significant change in the electrokinetic potential of erythrocytes is accompanied by a strong increase in lipid peroxidation upon 30 min incubation with PLA_2. We observe that increasing concentration of PLA_2 promotes more TBARS products in human erythrocytes. The Vipoxin electrostatic interaction has similar effect on erythrocyte membrane (as in the case of PLA_2) where a blebbing effect in higher concentrations of treatment is viewed [48]. VAC and Vipoxin enhance the net surface charge density of erythrocyte membranes and decrease the lipid peroxidation of the membranes at fixed 50 nM dose.

Viper toxins alter the passive electrical properties of the membrane. The anion-exchange function of Band 3 is altered with enhancement in proton transport and conductivity of erythrocytes by PLA_2 and Vipoxin treatments. VAC induces an increase in surface electrical charge due to increase in conductivity through the membrane, but reduces the proton efflux because of low pI=4.3 of the macromolecules. The reported results open perspectives to a further investigation of the surface electrical charge of the membrane after viper toxins treatment to shed light on the molecular mechanisms driving the mechanisms of inflammation and neurodegenerative diseases.

5. Conclusion

Microelectrophoresis approach allows for the following conclusions on the effects of purified components of Vipoxin on the electrokinetic potential of erythrocytes to be reported: *(i)* No significant change of the surface electrical charge and strong increase in osmotic fragility (570 nm) upon 50 nM PLA_2 dose. *(ii)* Increased stability of the system in the presence of 50 nM VAC or 50 nM Vipoxin due to exposure of additional negative charges at dimeric interface of Band 3 of the membrane; *(iii)* The electrokinetic potential of erythrocytes upon 50 nM of VAC or Vipoxin treatment showed that the viper components are used for causing higher net negative electrical charges on the erythrocyte surface impeding the process of aggregation of the cells due to a higher osmotic fragility (544 nm). This broadens the perspectives of biomacromolecules research using a novel physico-chemical properties of the erythrocyte membrane and points out the role of VAC and Vipoxin in the enhancement of stability of the cells for time before erythrocyte aggregation.

The protective effect of lower doses of viper toxins observed by the lipid peroxidation of erythrocytes relates to the non-specific electrostatic interactions. The reported results open new perspectives to further investigation of the role of the type of lipids and lipid domains on the peroxidation related processes in viper toxin-exposed erythrocytes with the purpose of clarifying the molecular mechanisms driving its protective role.

Viper toxins accelerate the proton efflux and conductivity in the erythrocyte suspension following the effectiveness line: PLA_2>Vipoxin>VAC. By providing knowledge on the proton transport through Band 3 of the erythrocyte membranes in the presence of viper toxins the reported results may serve for clarifying the mechanism of its biologically active action.

Conflict of interest

No conflicts of interest to report.

Author contributions

V. D. – conceptualization, methodology, validation, formal analysis, investigation, data curation, visualization, writing- original draft preparation, review and editing, project administration**,** P. R. A. – validation, formal analysis, visualization, writing - original draft preparation, review and editing, S. P. S. – reviewing the manuscript .

Acknowledgments

This work was supported by the Bulgarian National Fund of Scientific Research (Grant KP-06-N38/14/2019). The authors thanks for the generous gift of vipoxin and its separated components from Prof. Dr. S. D. Petrova.

Abbreviations

EPM– electrophoretic mobility;

ζ– electrokinetic (zeta) potential;

σ– surface charge density (surface electrical charge);

æ – electrical conductivity;

HEPES– N-(2-Hydroxyethyl) piperazine-N′- (2-ethanesulfonic acid);

PBS– phosphate – buffered saline;

583 PLA_2– phospholipase A_2 (Vipoxin basic component);

584 VAC – Vipoxin acidic component;

585 NU – neuraminidase;

586 Hct – hematocrit;

587 OF – osmotic fragility;

588 MDA– malondialdehyde;

589 TBA– 2-thiobarbituric acid;

590 TBARS– thiobarbituric acid reactive substances.

591

592 **References**

593

594 [1] A. Ramamoorthy, S. Thennarasu, D-K. Lee, A. Tim, L. Maloy, Solid state NMR
595 investigation of the membrane-disrupting mechanism of Antimicrobial Peptides MSI-78
596 and MSI-594 derived from magainin 2 and melittin, Biophysical Journal, 91 (2006)
597 206-216, doi: 10.1529/biophysj.105.073890.

598 [2] A. Bhunia, P.N. Domadia, S. Bhattacharjya, Structural and thermodynamic analyses of
599 the interaction between melittin and lipopolysaccharide, Biochimica et Biophysica Acta,
600 1768 (2007) 3282-3291, doi:10.1016/j.bbamem.2007.07.017.

601 [3] J. Hong, X. Lu, Z. Deng, S. Xiao, B. Yuan, K. Yang, How melittin inserts into cell
602 membrane: Conformational changes, inter-peptide cooperation, and disturbance on the
603 membrane, Molecules, 24 (2019) 1775, doi: 10.3390/molecules24091775.

604 [4] M.C. de Araujo Melo, C.G. Rodrigues, L. Pol-Fachin, *Staphylococcus aureus* δ-toxin in
605 aqueous solution: Behaviour in monomeric and multimeric states, Biophysical Chemistry,
606 227 (2017) 21-28, http://doi.org/10.1016/j.bpc.2017.05.015.

607 [5] M.N. Karemore, J.G. Avari, Alteration in zeta potential of erythrocytes in preeclampsia
608 patients, Nidhi Sharma, IntechOpen.85952, doi:10.5772/intechopen.85952.

609 [6] H.P. Fernandes, C.L. Cesar, M.L. Barjas-Castro, Electrical properties of the red blood
610 cell membrane and immunohematological investigation, Revista Brassiliera de
611 Hematologia e Hemoterapia, 33(4) (2011) 297-301, doi:10.5581/1561-8484-20110080.
612 [7] V.V. Revin, N.V. Gromova, E.S. Revina, M.I. Martynova, A.I. Seikina, N.V. Revina,
613 O.G. Imarova, I.N. Solomadin, A.Yu. Tychkov, N. Zhelev, Role of membrane lipids in the
614 regulation of erythrocytic oxygen-transport function in cardiovascular diseases, BioMed
615 Research International, vol. 2016 (2016), article ID 3429604,
616 http://dx.doi.org/10.1155/2016/3429604.
617 [8] C. Leonard, H. Pollet, C. Vermylen, N. Gov, D. Tyteca, M-P. Mingeot-Leclecq,
618 Tunning of differential order between submicrometric domains and surrounding membrane
619 upon erythrocyte reshaping, Cell Physiology and Biochemistry, 48 (2018) 2563-2582,
620 doi:10.1159/000492700.
621 [9] R.H. Fang, B.T. Luk, C-M J. Hu, L. Zhang, Engineered nanoparticles mimicking cell
622 membranes for toxin neutralization, Advanced Drug Delivery Reviews, 90 **(**2015) 69-80,
623 doi:10.1016/j.addr.2015.04.001.
624 [10] R.A. Campbell, E.B.Watkins, V. Jagalski, A. Åkesson-Runnsjö, Key Factors
625 Regulating the Mass Delivery of Macromolecules to Model Cell Membranes: Gravity and
626 Electrostatics, ACS Macro Letters, 3(2) (2014) 121-125,
627 https://doi.org/10.1021/mz400551h.
628 [11] R.M. Kini, Excitement ahead: structure, function and mechanism of snake venom
629 phospholipase A2 enzymes, Toxicon, 42 (2003) 827-840,
630 doi:10.1016/j.toxicon.2003.11.002.
631 [12] C.Y. Koh, R.M. Kini, From snake venom toxins to theurapeutics-cardiovascular
632 examples, Toxicon, 59(4) (2012) 497-506, doi:10.1016/j.toxicon.2011.03.017.
633 [13] S.L. Da Silva, E.G. Rowan, F. Albericio, R.G. Stábeli, L.A. Calderon, A.M. Soares,
634 Animal toxins and their advantages in biotechnology and pharmacology, BioMed Research
635 International, 2014 (2014) Art No ID 951561, https://doi.org/10.1155/2014/951561.

636 [14] N. Chen, S. Xu, Y. Zhang, F. Wang. Animal protein toxins: origin and therapeutic
637 applications, Biophysics Reports, 4(5) (2018) 233-242,
638 https//doi.org/10.1007/s41048-018-00667-x.
639 [15] A.M. Soares, J.P. Zuliani, Toxins and animal venoms and inhibitors: Moleculare and
640 biotechnological tools useful to human and animal health, Current Topics in Medicinal
641 Chemistry, 19(21) (2019) 1868-1871, doi:10.2174/1568026619211910241148 42.
642 [16] K. Balashev, V. Atanasov, M. Mitewa, S. Petrova, T. Bjørnholm, Kinetics of
643 degradation of dipalmitoylphosphatidylcholine (DPPC) bilayers as a result of vipoxin
644 phospholipase A2 activity: an atomic force microscopy (AFM) approach, Biochimica et
645 Biophysica Acta 1808(1) (2011) 191-198, http://dx.doi.org/10.1016/j.bbamem.2010.10.008.
646 [17] S.D. Petrova, V.N. Atanasov, K. Balashev, Vipoxin and its components: structure
647 –function relationship, in Ch. Z. Christov, T. Karabencheva-Christova (Eds.), Advances in
648 Protein Chemistry and Structural Biology, vol. 87, Structural and Mechanistic
649 Enzymology: Bringing together experiments and computing, Academic Press, San Diego,
650 USA, 2012, pp. 117-155.
651 [18] J. Doumanov, K. Mladenova, T. Topouzova-Hristova, S. Stoitsova, S. Petrova,
652 Effects of vipoxin and its components on HepG2 cells, Toxicon, 94 (2015) 36-44,
653 http://dx.doi.org/10.1016/j.toxicon.2014.12.009.
654 [19] R. Glaser, J. Donath, Stationary ionic states in human red blood cells,
655 Bioelectrochemistry and Bioenergetics, 13 (1984) 71-83.
656 [20] S.E. Lux, K.M. John, R.R. Kopito, H.F. Lodish, Cloning and characterization of
657 band 3, the human erythrocyte anion-exchange protein (AE1), Proceedings of the National
658 Academy of Sciences USA, 86 (1989) 9089-9093, https://doi.org/10.1073/pnas.86.23.9089
659 [21] A.C. Kalli, R.A.F. Reithmeier, Interaction of the human erythrocyte Band 3 anion
660 exchanger 1 (AE1, SLC4A1) with lipids and glycophorin A: Molecular organization of the
661 Wright (Wr) blood group antigen, PLoS Computational Biology, 14(7) (2018) e1006284,
662 https://doi.org/10.1371/journal.pcbi.1006284.

663 [22] E. Taşkin, S. Çelik, D.M. Yavuz, F. Kara, Investigation of relationship between
664 erythrocyte sedimentation rate and erythrocyte indices, *Kafkas Journal of Medical*
665 *Sciences*, 9(2) (2019) 87-89, doi:10.5505/kjms.2019.67934.
666 [23] A. Valadão Cardoso, An experimental erythrocyte rigidity index (R_i) and its
667 correlations with Transcranial Doppler velocities (TAMMV), golling Pulsatility Index PI,
668 hematocrit, hemoglobin concentration and red cell distribution width (RDW), *PLoS ONE*
669 15(2) (2020) e0229105, https://doi.org/10.1371/journal.pone.0229105.
670 [24] B. Tchorbanov, E. Grishin, B. Alexiev, Y. Ovchinnikov, A neurotoxic complex
671 from the venom of the Bulgarian viper (Vipera ammodytes ammodytes) and partial amino
672 acid sequence of the toxic phospholipase A2, Toxicon 16(1) (1978) 37-44,
673 doi:10.1016/0041-0101(78)90058-2.
674 [25] D.A. Six and E.A. Dennis, The expanding superfamily of phospholipase A(2)
675 enzymes: classification and characterization, Biochimica et Biophysica Acta 1488(1-2)
676 (2000) 1-19, doi:10.1016/s1388-1981(00)00105-0.
677 [26] E.A. Dennis, J. Cao, Y-H. Hsu, V. Magrioti, G. Kokotos, Phospholipase A2
678 enzymes: physical structure, biological function, disease implication, chemical inhibition,
679 and therapeutic intervention, Chemical Reviews, 111(10) (2011) 6130-6185,
680 doi:10.1021/cr200085w.
681 [27] D.N. Georgieva, N. Genov, K.R. Rajashankar, B. Aleksiev, C. Betzel, Spectroscopic
682 investigation of phenolic groups ionization in the vipoxin neurotoxic phospholipase A_2:
683 Comparison with the X-ray structure in the region of the tyrosyl residues, Spectrochimica
684 Acta Part A, 55(1999) 239-244.
685 **[**28**]** T. Matsui, S. Kamata, K. Ishii, T. Maruno, N. Ghanem, S. Uchiyama, K. Kato, A.
686 Suzuki, N. Oda-Ueda, T. Ogawa, Y. Tanaka, SDS-induced oligomerization of
687 Lys49-phospholipase A_2 from snake venom, Scientific Reports, 9 (2019) 2330,
688 https://doi.org/10.1038/s41598-019-38861-8.
689 [29] T.W. Yau, R.P. Kuchel, J.M.S. Koh, D. Szekely, P.W. Kuchel, Cytoskeletal
690 rearrangements in human red blood cells induced by snake venoms: light microscopy of

691 shapes and NMR studies of membrane function, Cell Biology International, 36 (2012)
692 87-97, doi:10.1042/CBI20110012.
693 [30] S. Banumathi, K.R. Rajashankar, C. Nöetzel, B. Alexiev, T.P. Singh, N. Genov, C.
694 Betzel, Structure of the neurotoxic complex vipoxin at 1.4 Å resolution, Acta
695 Crystallographica Section D: Structural Biology, 57(Pt 11) (2001) 1552-1559,
696 doi:10.1107/s0907444901013543.
697 [31] Y. Devedjiev, A. Popov, B. Atanasov, H.D. Bartunik, X-ray structure at 1.76 Å
698 resolution of a polypeptide phospholipase A_2 Inhibitor, Journal of Molecular Biology, ,
699 266(1) (1997) 160-72, doi:10.1006/jmbi.1996.0778.
700 [32] M. Perbandt, J.C. Wilson, S. Eschenburg, I. Mancheva, B. Aleksiev, N. Genov, P.
701 Willingmann, W. Weber, T.P. Singh, Ch. Betzel, Crystal structure of vipoxin at 2.0 Å: an
702 example of regulation of a toxic function generated by molecular evolution, FEBS Letters,
703 412 (1997) 573-577, https://doi.org/10.1016/S0014-5793(97)00853-3.
704 [33] C. Keith, D.S. Feldman, S. Deganello, J. Glick, K.B. Ward, E.O. Jones, P.B.
705 Sigler, The 2.5 Å crystal structure of a dimeric phospholipase A_2 from venom *Crotalus*
706 *atrox*, Journal of Biological Chemistry, 256 (1981) 8602-8607.
707 [34] J.E. Freedman, S.H. Snyder, Vipoxin A protein from Russell's viper venom with
708 high affinity for biogenic amine receptors, Journal of Biological Chemistry, 256 (24)
709 (1981) 13172-13179.
710 [35] K.A. Runas, N. Malmstadt, Low levels of lipid oxidation radically increase the
711 passive permeability of lipid bilayers, Soft Matter, 11 (2015) 499-505,
712 https://doi.org/10.1039/C4SM01 478B.
713 [36] A. Ayala, M.F. Muñoz, S. Argüelles, Lipid peroxidation: Production, metabolism,
714 and signalling mechanisms of malondialdehyde and 4-hydroxy-2-nonenal, Oxidative
715 medicine and Cellular Longevity, vol.2014 (2014), Article ID 360438,
716 https://dx.doi.org/10.1155/2014/360438.

717 [37] C. Pertibois, G. Déléris, Evidence that erythrocytes are highly susceptible to exercise
718 oxidative stress: FT-IR spectrometric studies at the molecular level, Cell Biology
719 International, 29(8) (2005) 709-716, https://doi.org/10.1016/j.cellbi.2005.04.007.
720 [38] T.M. Tsubone, M.S. Baptista, R. Itri, Understanding membrane remodelling initiated
721 by photosensitized lipid oxidation, Biophysical Chemistry, 254 (2019) 106263,
722 https://doi.org/10.1016/j.bpc.2019.106263.
723 [39] P.K. Smith, R.I. Krohn, G.T. Hermanson, A.K. Mallia, F.H. Gartner, M.D.
724 Provenzano, E.K. Fujimoto, N.M. Goeke, B.J. Olson, D.C. Klenk, Measurement of portein
725 using bicinchoninic acid, Analytical Bochemistry, 150 (1985) 76-85,
726 doi:10.1016/0003-2697(85)90442-7.
727 [40] I. Mancheva, T. Kleinschmidt, B. Alexiev, G. Braunitzer, Sequence homology
728 between phospholipase and its inhibitor in snake venom. The primary structure of
729 phospholipase A_2 of vipoxin from the venom of the Bulgarian viper (Vipera ammodytes
730 ammodytes, Serpentes), Biological Chemistry Hoppe Seyler, 368 (1987) 343-352,
731 doi:10.1515/bchm3.1987.368.1.343.
732 [41] B. Tchorbanov, B. Alexiev, A simple procedure for the isolation of Vipoxin – a
733 neurotoxin with phospholipase A_2 activity from the venom of the Bulgarian viper (Vipera
734 ammodytes), Journal of Applied Biochemistry, 3 (1981) 558-561.
735 [42] J. Rifkind, K. Araki, E. Hadley, The relationship between the osmotic fragility of
736 human erythrocytes and cell age. Archives in Biochemistry and Biophysics, 222 (1983)
737 582-589, doi:10.1016/0003-9861(83)90556-8.
738 [43] F. Men, A.I. Alayash, Determination of extinction coefficients of human
739 hemoglobin in various redox states, Analytical Chemistry, 521(2017) 11-19,
740 doi:10.1016/j.ab.2017.01.002.
741 [44] G.M. Barrow, Physical Chemistry. 1996, McGraw – Hill: Boston, Massachusetts.
742 [45] S. McLaughlin, Electrostatic Potentials at membrane-solution interfaces, Current
743 Topics in Membranes and Transport, 9 (1977) 71-144.

[46] B. Halliwell, J.M. Gutterdge, in B. Halliwell and J.M.C Gutteridge (Eds.), Free Radicals in Biology and Medicine, 1999. 3rd Edition, Oxford University Press, Oxford: p. 1-25.

[47] S. Lepke, J. Heberle, H. Passow, 10 The Band 3 protein: Anion exchanger and anion-proton cotrnasporter, in I. Bernhardt, J.C. Ellory (Eds.), Red cell membrane transport in health and disease, Springer, 2003, pp. 221-252.

[48] R. Georgieva, K. Mircheva, V. Vitkova, K. Balashev, T. Ivanova, C. Tessier, K. Koumanov, P. Nuss, A. Momchilova, G. Staneva, Phospholipase A2-Induced Remodeling Processes on Liquid-Ordered/Liquid-Disordered Membranes Containing Docosahexaenoic or Oleic Acid: A Comparison Study, Langmuir 32(7) (2016) 1756-1770, doi:10.1021/acs.langmuir.5b03317.

[49] S. Stankowski, Surface charging by large multivalent molecules. Extending the standard Gouy-Chapman treatment, Biophysical Journal. 60(2) (1991) 341-351, doi:10.1016/S0006-3495(91)82059-8.

[50] Y-X. Huang, Z-J Wu, J. Mehrishi, B-T Huang, X-Y Chen, X-J Zheng, W-J Liu, M. Luo, Human red blood cell aging: correlative changes in surface charge and cell properties, Journal of Cellular and Molecular Medicine, 15(12) (2011) 2634-2642, doi:10.1111/j.1582-4934.2011.01310.x.

[51] M.G. Salgo, F.P. Corongui, A. Sevanian, Enhanced interfacial catalysis and hydrolytic specifity of phospholipase A1, Archives of Biochemistry and Biophysics, 304 (1993) 123-132.

[52] N.M. Litvinko, L.A.Skorosteskaya, D.O. Gerlovsky, The interaction of phospholipase A_2 with oxidized phospholipids at the lipid-water surface with different structural organization, Chemistry and Physics of Lipids, 211(2018) 44-51.

Figure Legends

Figure 1. Osmotic fragility of erythrocytes in the presence of viper toxins. (**A**) Osmotic fragility changes in erythrocytes in the presence of fixed concentrations of PLA_2, VAC and Vipoxin after incubation *in vitro* in NaCl solutions. Control samples contain saline instead of the toxin (0% hemolysis). (**B**) Effect of fixed concentrations of 50 nM of PLA_2, VAC and Vipoxin treatments on Hematocrit (average value ± SD of 5-7 independent repetitions, 3 independent experiments) of erythrocytes suspended in PBS, pH 7.4. Values of $p<0.05$ are considered significant.

Figure 2. Electrokinetic properties of erythrocytes in the presence of Neuraminidase. (**A**) Erythrocytes incubation without or in the presence of neuraminidase (NU) for 2 h at 37 ^oC. C_o – electrophoretic mobility **(**EPM) of control erythrocytes, measured immediately after washing of erythrocytes; C_1 – EPM of erythrocytes incubated for an hour without neuraminidase in Hepes buffered saline (25 mM Hepes, 130 mM NaCl, 3.7 mM KCl, 0.25 mM $CaCl_2$, pH 7.5); EPM of erythrocytes after 25 nM PLA_2 treatment without or in the presence of 10 mU and 20 mU neuraminidase, respectively; EPM of erythrocytes upon different concentrations of neuraminidase treatment (30 mU, 40 mU and 50 mU NU) in the presence of 50 nM, 80 nM and 100 nM PLA_2, respectively. The data are expressed as mean ± SD. Values of $p<0.05$ are considered significant. * $p=0.02$ or $p=0.013$, compared to the untreated control. (**B**) Zeta potential of erythrocytes after pre-incubation upon treatment at different concentrations of neuraminidase (NU).C_{60} – ζ potential of erythrocytes incubated for an hour without neuraminidase in Hepes buffered saline (25 mM Hepes, 130 mM NaCl, 3.7 mM KCl, 0.25 mM $CaCl_2$, pH 7.5); Erythrocytes are pre-incubated with neuraminidase (NU) at 1 h at 37 ^oC; Influence of PLA_2 treatments as followed: 10 mU NU + 25 nM PLA_2; 20 mU NU + 25 nM PLA_2; 30 mU NU + 50 nM PLA_2; 40 mM NU + 80 nM PLA_2 ; 50 mU + 100 nM PLA_2.ζ potential of erythrocytes upon upper NU treatments in the presence of different concentrations of PLA_2 exposure. Values of $p<0.05$ are considered significant. *** $p<0.001$, compared to the control without NU.

Figure 3. Zeta potential of erythrocytes in the presence of viper toxins. Zeta potential of human erythrocytes upon Vipoxin (**A**), PLA_2 (**B**) and VAC (**C**) treatments. Medium contains Hepes buffered saline. Data are means ± SD of three - seven independent experiments. *** $p<0.001$, compared to the control without viper toxins.

Figure 4. Surface electrical charge of erythrocytes in the presence of viper toxins. Surface electrical charge of erythrocytes in the presence of 50 nM of phospholipase A_2 (PLA_2), 50 nM Vipoxin acidic component (VAC) and 50 nM Vipoxin in suspending

medium of Hepes buffered saline. Values of each group present the mean ± SD of 5 independent experiments. *** $p<0.001$, compared to the untreated control.

Figure 5. Lipid peroxidation of erythrocytes in the presence of viper toxins. Lipid peroxidation in erythrocytes as a function of different concentrations of (**A**) phospholipase A_2 (PLA_2); Data are expressed as mean ± SD, 3 independent measurements with n = 3 repetitions. *** $p<0.001$, compared to the control samples without PLA_2. (**B**) Fixed concentrations of 50 nM of Phospholipase A_2, Vipoxin acidic component (VAC) and Vipoxin; Values of $p<0.05$ are considered significant. Suspending medium consist**s** of phosphate buffered saline (PBS). The second control of 50 mM H_2O_2 represents the maximal value of TBARS products in dependence of time of incubation (A: 5 min or 30 min at 37 ^oC; B: 1 hour at 37 ^oC).

Figure 6. H^+-Cl^- co-transport and conductivity in erythrocytes containing PLA_2. (**A**) Extracellular proton concentration (H^+_{ext}) as a function of time (s), calculated from the recorded ΔpH changes induced by sudden jumps of the extracellular proton concentration of erythrocytes in Sucrose, salt-free medium (NaOH), pH 7.4, in the presence of different concentrations of PLA_2. (**B**) The initial slopes of linear fit curve of ΔpH changes in erythrocyte membranes without or in the presence of different doses of PLA_2. (**C**) Conductivity measurements as a function of time (s) in erythrocytes suspended in Sucrose, salt-free medium (NaOH), pH 7.4, in the presence of different concentrations of PLA_2. (**D**) The initial slopes of linear fit curve of Δæ changes in erythrocyte membranes without or in the presence of different doses of PLA_2.

Figure 7. H^+-Cl^- co-transport and conductivity in erythrocytes containing viper toxins. (**A**) Extracellular proton concentration (H^+_{ext}) as a function of time (s), calculated from the recorded ΔpH changes induced by sudden jumps of the extracellular proton concentration of erythrocytes in Sucrose, salt-free medium (NaOH), pH 7.4, in the presence of fixed concentrations of 50 nM PLA_2, 50 nM VAC and 50 nM Vipoxin, respectively. (**B**) The initial slopes of linear fit curve of ΔpH changes in erythrocyte membranes without or in the presence of fixed concentrations of 50 nM doses of viper toxins. (**C**) Conductivity measurements as a function of time (s) in erythrocytes suspended in Sucrose, salt-free medium (NaOH), pH 7.4, in the presence of fixed concentrations of 50 nM PLA_2, 50 nM VAC and 50 nM Vipoxin, respectively. (**D**) Initial slopes of linear curve fit of Δæ changes in

erythrocyte membranes without or in the presence of fixed concentrations of 50 nM doses of viper toxins.

Supplementary Figure 1. Protein components of neurotoxin, isolated from Vipera ammodytes meridionalis. (**A**) Electrophoretic analysis of protein components in 12% polyacrylamide gel under non-reducing conditions (Vipera ammodytes meridionalis venom). Profiles of the protein fractions are presented. M – marker. (**B**) Immunoblot from control and experimental mouse animals after Vipoxin treatment – neurotoxin isolated from Vipera ammodytes meridionalis: VAC – Vipoxin acidic component, M – Marker, PLA2 – phospholipase A2, NT – untreated animal). A reaction is found in the brain of all animals where the untreated (NT) and treated with Vipera ammodytes meridionalis venom are noticed at a level of ~28 kDa, which is the Mr of Vipoxin.

Figures

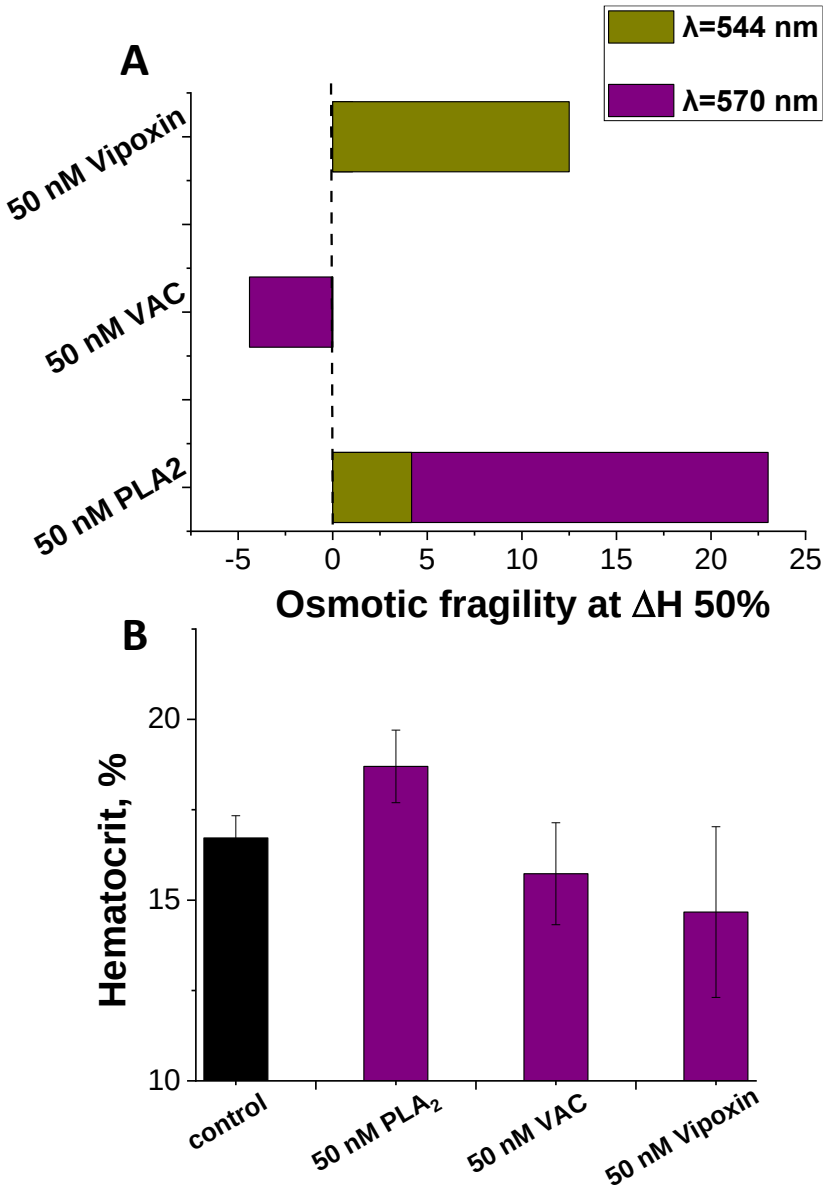

Figure 1

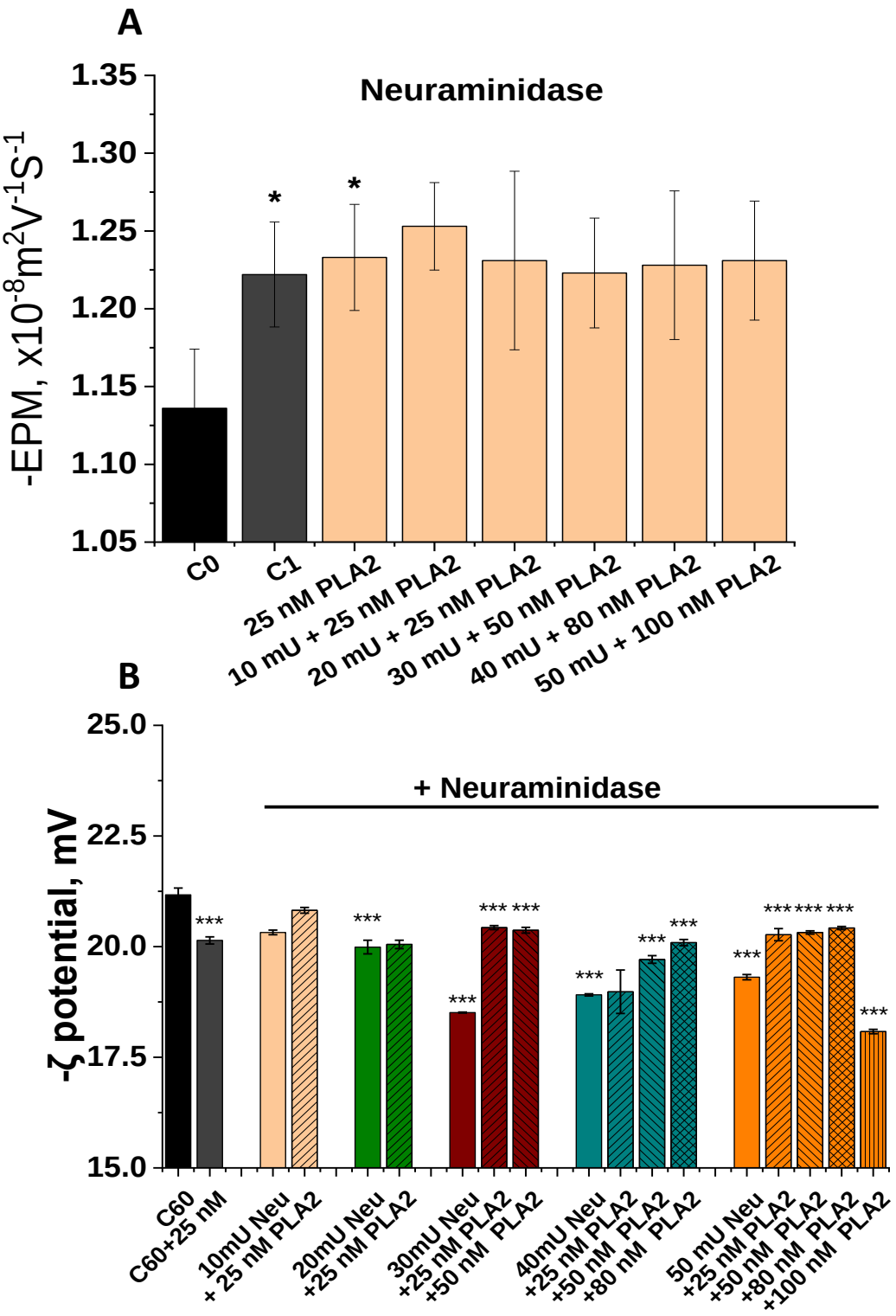
A
Neuraminidase
-EPM, x10-8m2V-1S-1
1.35
1.30
1.25
1.20
1.15
1.10
1.05
*
*
C0
C1
25 nM PLA2
10 mU + 25 nM PLA2
20 mU + 25 nM PLA2
30 mU + 50 nM PLA2
40 mU + 80 nM PLA2
50 mU + 100 nM PLA2
B
+ Neuraminidase
-ζ potential, mV
25.0
22.5
20.0
17.5
15.0
***
C60
C60+25 nM
10mU Neu + 25 nM PLA2
20mU Neu +25 nM PLA2
30mU Neu +25 nM PLA2 +50 nM PLA2
40mU Neu +25 nM PLA2 +50 nM PLA2 +80 nM PLA2
50 mU Neu +25 nM PLA2 +50 nM PLA2 +80 nM PLA2 +100 nM PLA2

Figure 2

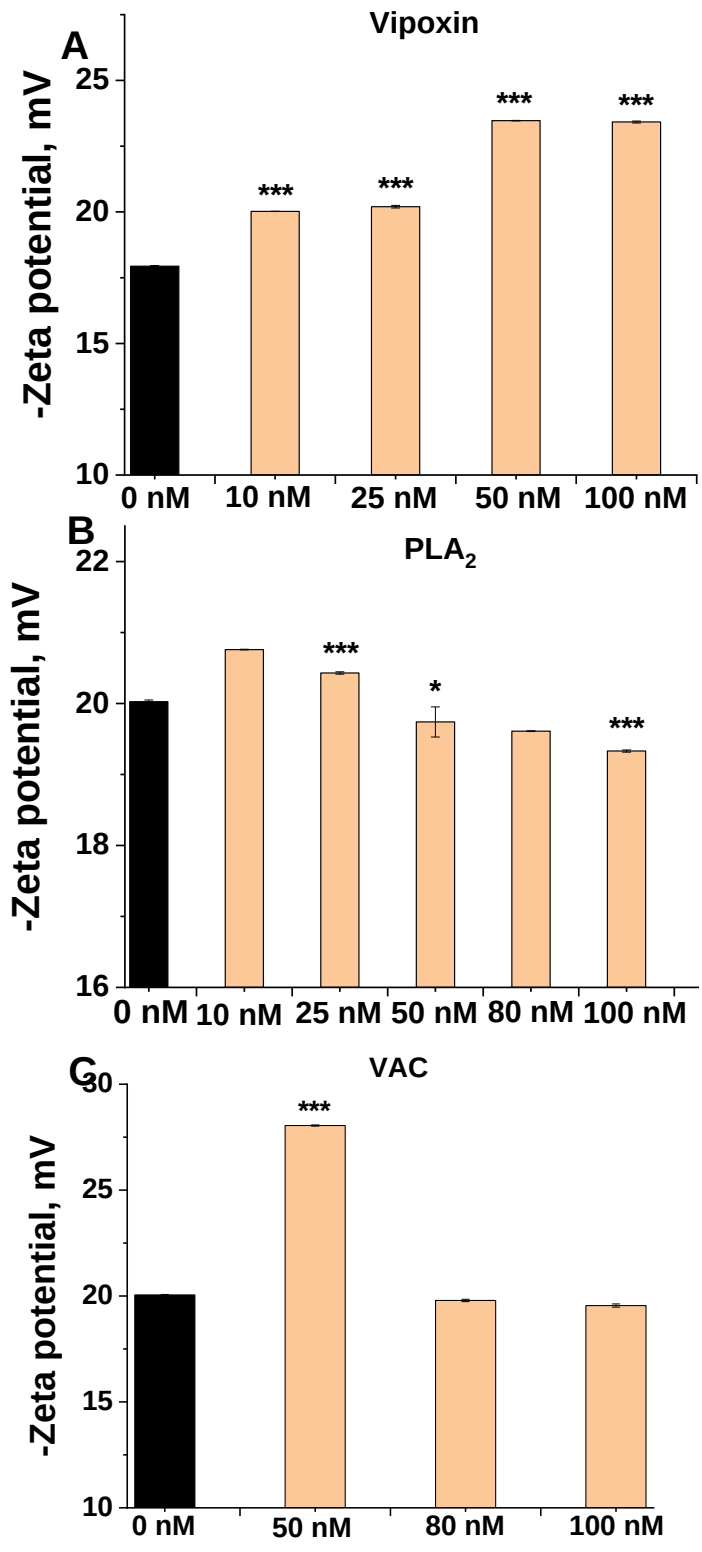
A
Vipoxin
-Zeta potential, mV
25
20
15
10
***
***
***
***
0 nM
10 nM
25 nM
50 nM
100 nM
B
PLA2
-Zeta potential, mV
22
20
18
16
***
*
***
0 nM
10 nM
25 nM
50 nM
80 nM
100 nM
C
VAC
-Zeta potential, mV
30
25
20
15
10
***
0 nM
50 nM
80 nM
100 nM

Figure 3

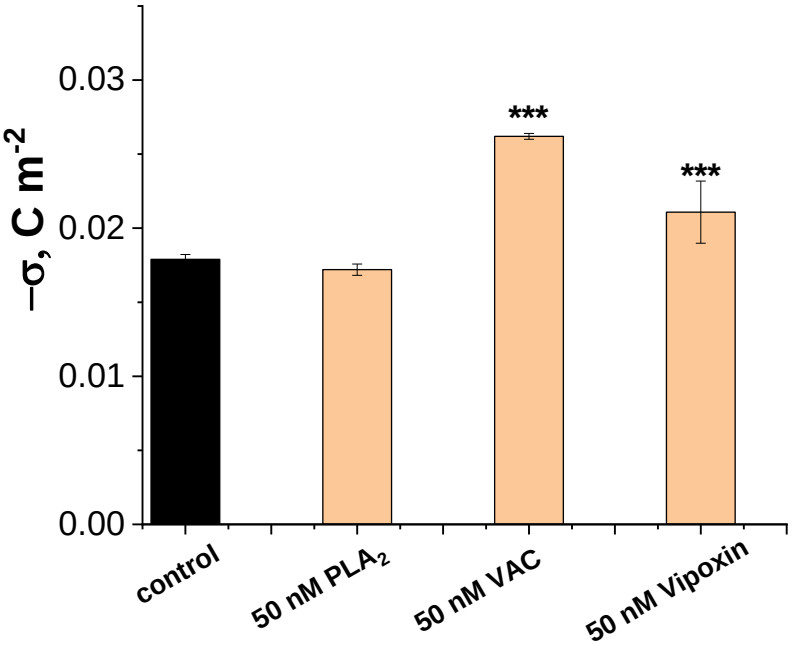

Figure 4

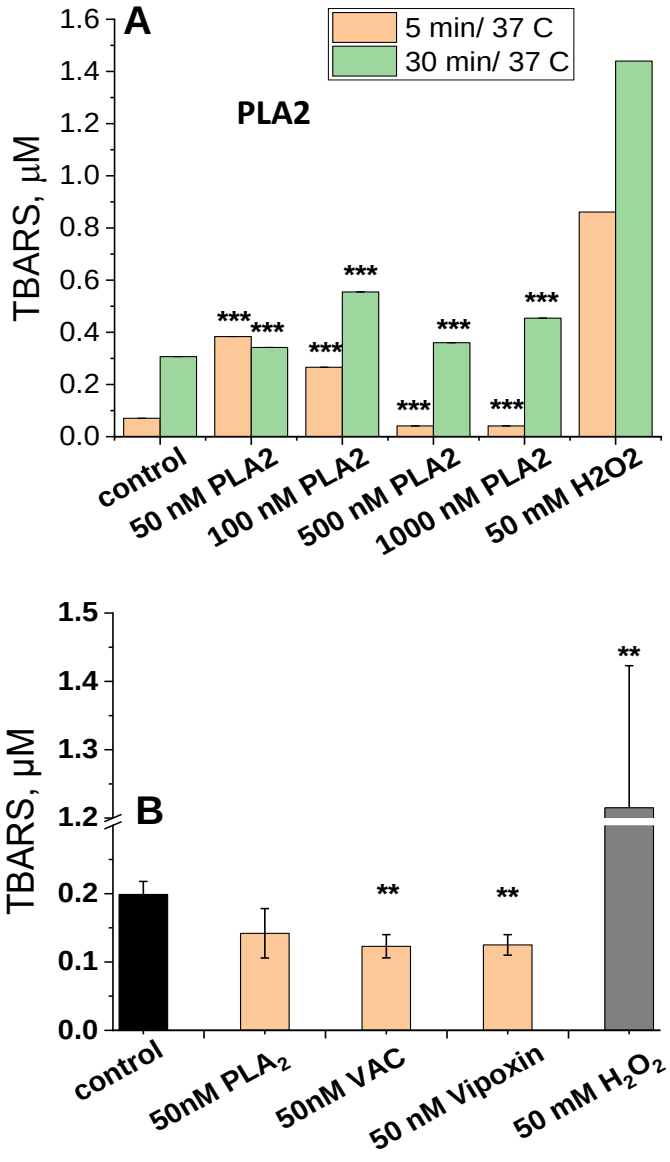
A
PLA2
5 min/ 37 C
30 min/ 37 C
TBARS, µM
1.6
1.4
1.2
1.0
0.8
0.6
0.4
0.2
0.0
***
control
50 nM PLA2
100 nM PLA2
500 nM PLA2
1000 nM PLA2
50 mM H2O2
B
TBARS, µM
1.5
1.4
1.3
1.2
0.2
0.1
0.0
**
control
50nM PLA2
50nM VAC
50 nM Vipoxin
50 mM H2O2

Figure 5

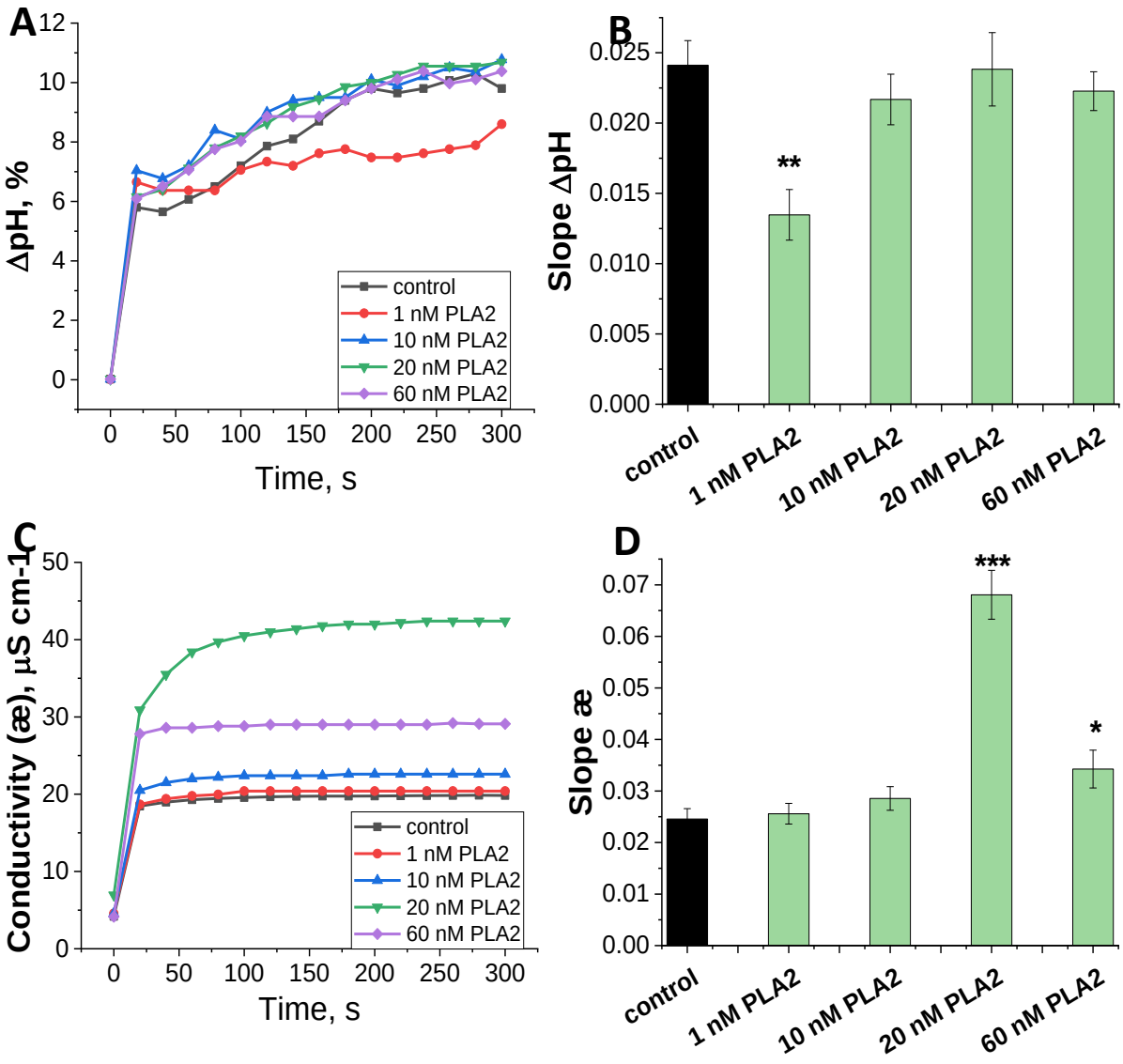
A
ΔpH, %
Time, s
control
1 nM PLA2
10 nM PLA2
20 nM PLA2
60 nM PLA2
B
Slope ΔpH
**
control
1 nM PLA2
10 nM PLA2
20 nM PLA2
60 nM PLA2
C
Conductivity (æ), µS cm-1
Time, s
control
1 nM PLA2
10 nM PLA2
20 nM PLA2
60 nM PLA2
D
Slope æ
***
*
control
1 nM PLA2
10 nM PLA2
20 nM PLA2
60 nM PLA2

Figure 6

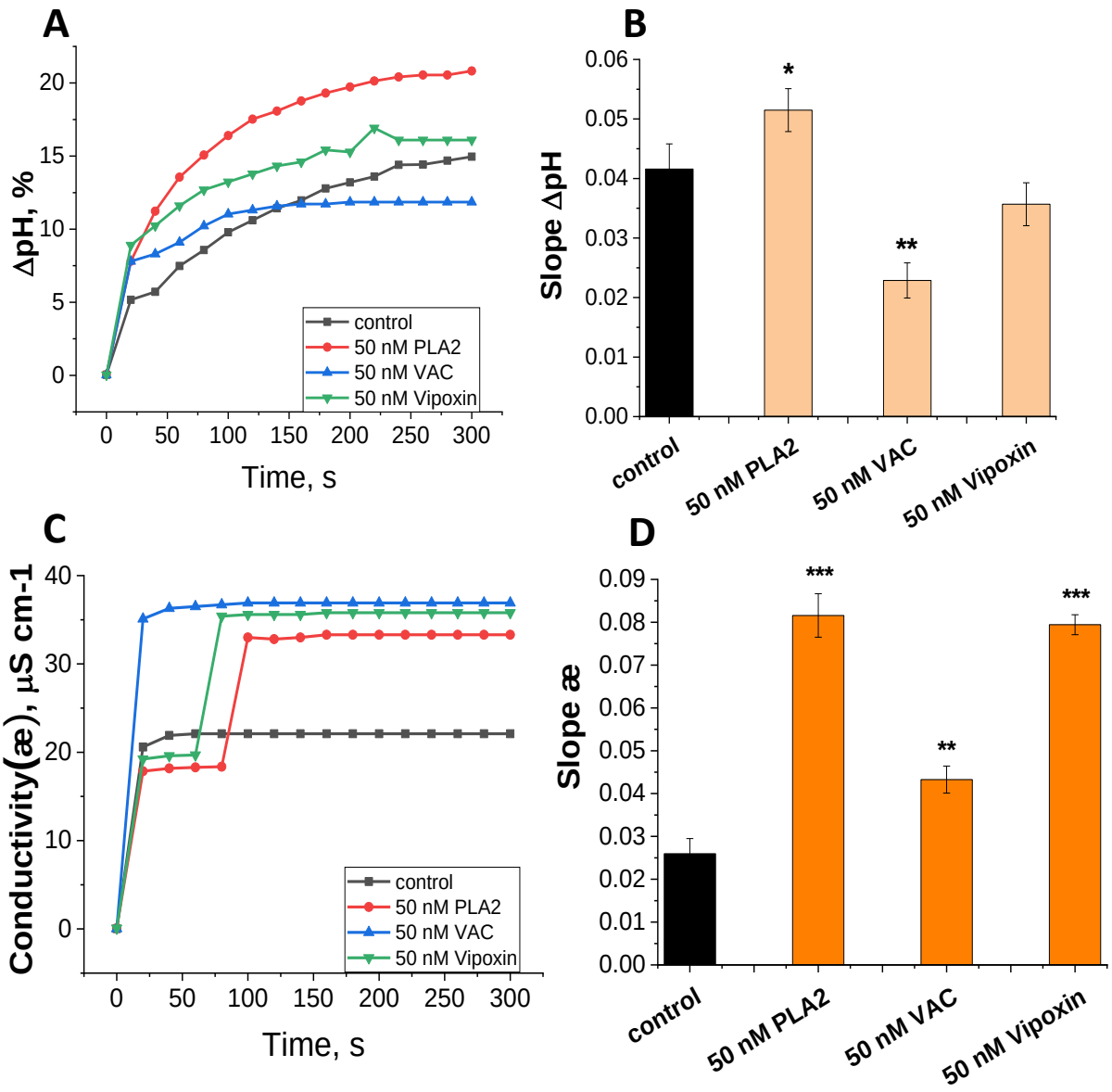
A
ΔpH, %
Time, s
control
50 nM PLA2
50 nM VAC
50 nM Vipoxin
B
Slope ΔpH
control
50 nM PLA2
50 nM VAC
50 nM Vipoxin
C
Conductivity(æ), µS cm-1
Time, s
control
50 nM PLA2
50 nM VAC
50 nM Vipoxin
D
Slope æ
control
50 nM PLA2
50 nM VAC
50 nM Vipoxin

Figure

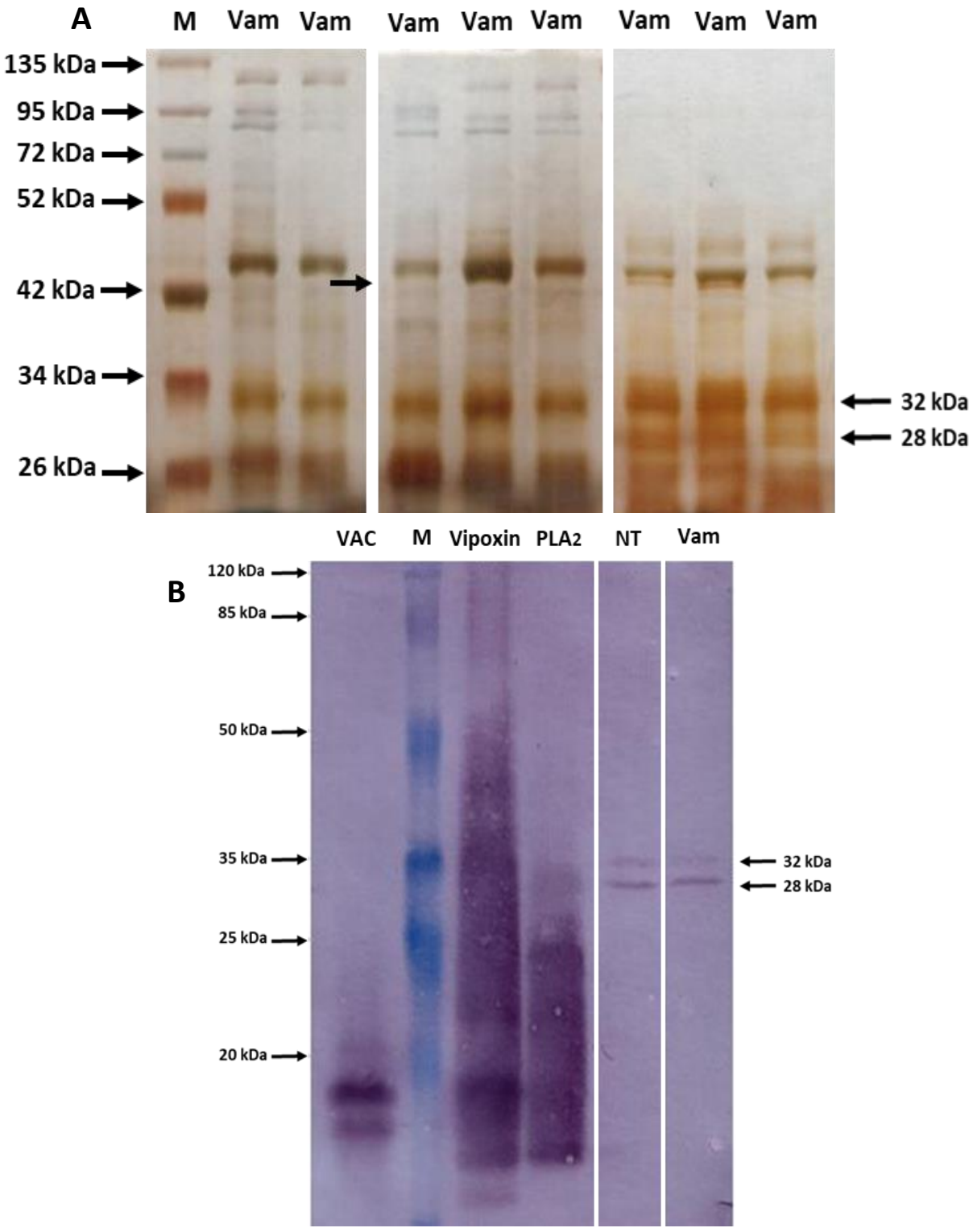

Suppl. Figure